



Published in final edited form as:

*Oncogene*. 2012 April 26; 31(17): 2129–2139. doi:10.1038/onc.2011.407.

## Manganese superoxide dismutase is a mitochondrial fidelity protein that protects Poly against UV-induced inactivation

Vasudevan Bakthavatchalu, M.V.Sc<sup>1</sup>, Swatee Dey, Ph.D.<sup>2</sup>, Yong Xu, Ph.D.<sup>1</sup>, Teresa Noel, B.S.<sup>1</sup>, Paiboon Jungsuwadee, Ph.D.<sup>1,3</sup>, Aaron K. Holley, Ph.D.<sup>1</sup>, Sanjit K. Dhar, Ph.D.<sup>1</sup>, Ines Batinic-Haberle, Ph.D.<sup>4</sup>, and Daret K. St Clair, Ph.D.<sup>1,\*</sup>

<sup>1</sup>Graduate Center for Toxicology, University of Kentucky, Lexington, KY 40536

<sup>2</sup>Proctor & Gamble, Cincinnati, OH 45202

<sup>3</sup>Department of Pharmacology and Toxicology, Husson University, Bangor, ME 04401

<sup>4</sup>Duke University Medical Center, Durham, NC 27705

### Abstract

Manganese superoxide dismutase is a nuclear encoded primary antioxidant enzyme localized exclusively in the mitochondrial matrix. Genotoxic agents, such as UV radiation, generates oxidative stress and cause mitochondrial DNA (mtDNA) damage. The mitochondrial DNA polymerase (Poly), a major constituent of nucleoids, is responsible for the replication and repair of the mitochondrial genome. Recent studies suggest that mitochondria contain fidelity proteins and MnSOD constitutes an integral part of the nucleoid complex. However, it is not known whether or how MnSOD participates in the mitochondrial repair processes. Using skin tissue from C57/BL6 mice exposed to UVB radiation, we demonstrate that MnSOD plays a critical role in preventing mtDNA damage by protecting the function of Poly. Q-PCR analysis shows an increase in mtDNA damage after UVB exposure. Immunofluorescence and immunoblotting studies demonstrate p53 translocation to mitochondria and interaction with Poly after UVB exposure. The mtDNA immunoprecipitation assay with Poly and p53 antibodies in p53<sup>+/+</sup> and p53<sup>-/-</sup> mice demonstrates an interaction between MnSOD, p53, and Poly. The results suggest that these proteins form a complex for the repair of UVB-associated mtDNA damage. The data also demonstrate that UVB exposure injures the mtDNA D-loop in a p53-dependent manner. Using MnSOD-deficient mice we demonstrate that UVB-induced mtDNA damage is MnSOD-dependent. Exposure to UVB results in nitration and inactivation of Poly, which is prevented by addition of the MnSOD mimetic Mn<sup>III</sup>TE-2-PyP<sup>5+</sup>. These results demonstrate for the first time that MnSOD is a fidelity protein that maintains the activity of Poly by preventing UVB-induced nitration and inactivation of Poly. The data also demonstrate that MnSOD plays a role along with p53 to prevent mtDNA damage.

Users may view, print, copy, download and text and data- mine the content in such documents, for the purposes of academic research, subject always to the full Conditions of use: [http://www.nature.com/authors/editorial\\_policies/license.html#terms](http://www.nature.com/authors/editorial_policies/license.html#terms)

\*Address correspondence to: Daret K. St. Clair, Ph.D., Graduate Center for Toxicology, University of Kentucky, 1095 VA Drive, HSRB 454, Lexington, KY 40536-0298, Phone: (859) 257-3720, FAX: (859) 323-1059, dstcl100@uky.edu.

### Conflict of Interest

The authors declare no conflict of interest.

## Keywords

Fidelity gene; Polymerase gamma; p53; MnSOD; Oxidative/nitrative stresses; Mn<sup>III</sup>TE-2-PyP<sup>5+</sup>

---

## Introduction

Ultraviolet (UV) radiation is a pro-oxidant and carcinogen that induces oxidative stress and DNA damage (Aitken *et al.*, 2007, Bickers and Athar 2006). UV irradiation leads to increased stabilization and accumulation of tumor suppressor protein p53 in the skin. The main contributing factor to non-melanoma skin cancer is UVB-induced signature mutations in the p53 gene (Brash *et al.*, 1991, Hall *et al.*, 1993, Liu *et al.*, 1994). N-acetyl cysteine (NAC), superoxide dismutase, and catalase mimetic attenuate UVB-induced p53 stabilization without altering the transcriptional activation and cell cycle arrest functions of p53, suggesting a role for oxidative stress in UVB-induced p53 stabilization and accumulation (Decraene *et al.*, 2004, Renzing *et al.*, 1996). Increased cellular stress by ROS triggers p53 translocation to mitochondria, leading to apoptosis and mtDNA repair (Mihara *et al.*, 2003, Mihara and Moll 2003, Waster and Ollinger 2009, Zhao *et al.*, 2002, Zhao *et al.*, 2005).

mtDNA is organized in the inner mitochondrial membrane as nucleoids. The nucleoids consist of mtDNA-protein macromolecular complexes containing 2–8 mtDNA molecules associated with various proteins such as mitochondrial transcription factor A (mTFA), a mitochondrial single-strand DNA-binding protein (mtSSB) and Pol $\gamma$  (Chen and Butow 2005, Garrido *et al.*, 2003, Legros *et al.*, 2004). mtDNA is more susceptible to UV-induced damage than nuclear DNA is because it lacks histone and an elaborate repair system (Brown *et al.*, 1979, Shokolenko *et al.*, 2009, Yakes and Van Houten 1997).

Pol $\gamma$  is the only known polymerase enzyme responsible for replication and repair of mtDNA (Bogenghagen *et al.*, 2001, Bolden *et al.*, 1977, Hubscher *et al.*, 1979, Longley *et al.*, 1998, Stuart *et al.*, 2004). The Pol $\gamma$  holoenzyme is a heterotrimer consisting of 1 catalytic subunit and 2 accessory subunits (Carrodegua *et al.*, 1999, Gray and Wong 1992, Yakubovskaya *et al.*, 2006). The Pol $\gamma$  catalytic subunit has polymerase and proof-reading activity for mtDNA replication, and dRP (5'-deoxyribose-5-phosphate) lyase activity for base excision repair. The accessory subunits bind nucleotide to mtDNA for faster replication, increased processivity and protection of the catalytic subunit from ROS-mediated oxidative damage (Johnson *et al.*, 2000). Pol $\gamma$  is susceptible to oxidative modifications due to the presence of 31 tyrosine residues in the catalytic subunit, including the two highly conserved tyrosine residues in the active site responsible for catalytic efficiency (Graziewicz *et al.*, 2002, Graziewicz *et al.*, 2004, Lewis *et al.*, 2006, Lim *et al.*, 2003, Van Goethem *et al.*, 2001).

UV irradiation triggers nitric oxide production in keratinocytes, which combines with superoxide to form the powerful oxidant peroxynitrite (Maglio *et al.*, 2005, Wu *et al.*, 2010). Inactivation of proteins by tyrosine nitration is regarded as a marker of nitrosative stress. The importance of nitration to protein structure or function depends on the location of tyrosine residues in the proteins; for example, its location in a loop or hydrophobic milieu such as the active site of an enzyme (Alvarez and Radi 2003).

ROS produced in mitochondria are detoxified by enzymatic and non-enzymatic antioxidant defense systems. The major constituents of the enzymatic system are MnSOD (Weisiger and Fridovich 1973), glutathione peroxidase (Esworthy *et al.*, 1997) and members of the thioredoxin family (Holmgren 1985). MnSOD forms the first line of defense against the superoxide produced in the mitochondria. Lack of MnSOD causes accumulation of oxidative mtDNA damage as well as inactivation of respiratory and Krebs cycle enzymes (Li *et al.*, 1995b, Melov *et al.*, 1999). Recent studies have identified MnSOD as a nucleoid complex component that may protect mtDNA and proteins associated with mtDNA from oxidative damage (Kienhofer *et al.*, 2009). Further MnSOD enzymatic activity is regulated by mitochondrial SIRT3 to maintain ROS levels and mitochondrial homeostasis (Ozden *et al.*, 2011, Tao *et al.*, 2010). We propose that epidermal cells use the following novel dual-step strategy to counteract a UVB insult involving tumor suppressor protein p53 and MnSOD 1) Damaged mtDNA recruit p53 to mitochondria where p53 might provide support to mitochondrial DNA polymerase Pol $\gamma$  in repairing the damaged mtDNA; and 2) MnSOD may act as a fidelity protein by interacting with Pol $\gamma$  and protecting it from oxidative stress-induced inactivation.

## Results

### UVB induces mtDNA damage in mouse skin

To assess mtDNA damage by UVB, we performed a time course study in which wild-type C57BL/6 mice were exposed to 5kJ/m<sup>2</sup> of UVB radiation. mtDNA isolated from skin at 1 and 24 hr after exposure to UVB was subjected to quantitative PCR analysis. The mtDNA damage was analyzed based on the difference in amplification due to blockage of the recombinant *Thermus thermophilus* (rTth) DNA polymerase by UVB-induced lesions. PCR negative control was used as a blank reference to eliminate background fluorescence. The relative amplification plot in Fig.1 shows a significant decrease in amplification of 10 kb mtDNA at 1 hr and 24 hr after UVB treatment compared to undamaged control template, indicating an increase in mtDNA damage. A quantitative analysis of lesions induced by UVB treatment in the 10 kb mtDNA is shown in Table 1. We normalized mtDNA copy number variation using fluorescence values from amplified short mtDNA fragments (117 bp), as there is a very low probability that UVB treatment will introduce a lesion in small mtDNA segments. This analysis indicates a significant increase in lesions at 1 hr and 24 hr after UVB treatment, suggesting mtDNA is highly prone to damage by UVB treatment.

### UVB induces p53 translocation to mitochondria in mice epidermal cells

We have previously observed p53 translocation to mitochondria in a multistage skin cancer model using a known mutagenic chemical initiator, 7,12-dimethyl-benz(a)-anthracene (DMBA), followed by repetitive treatment with the tumor promoter 12-*O*-tetradecanoylphorbol-13-acetate (TPA), which is a known tumor promoter (Zhao *et al.*, 2002). It has also been shown that p53 translocated into mitochondria after exposure to a stress inducing agent including ionizing radiation (Vaseva and Moll 2009). To determine whether UVB-induced mtDNA damage triggers p53 translocation to mitochondria *in vivo*, skin mitochondrial fractions devoid of cytosolic and nuclear contamination were prepared from mouse skin by a sucrose density gradient ultracentrifugation process after UVB

treatment and subjected to immunoblot analysis. As shown in Fig. 2A & 2B, the p53 level increased significantly in both whole skin lysates and mitochondrial fractions at 1 hr and at 24 hr after UVB treatment. The absence of cytosolic and nuclear contamination was confirmed by immunoblotting of the mitochondrial fractions with antibodies against cytosolic and nuclear marker proteins I $\kappa$ B $\alpha$  and PCNA, respectively.

### **UVB enhances physical interaction of p53 with Pol $\gamma$ and mtDNA, and the role of p53 in Pol $\gamma$ and mtDNA interaction**

Previous studies have shown that p53 can directly interact with Pol $\gamma$  and mtDNA and enhance Pol $\gamma$  repair efficiency (Achanta *et al.*, 2005, Bakhanashvili *et al.*, 2008, Heyne *et al.*, 2004). Here, we tested whether UVB could enhance p53 interaction with Pol $\gamma$  and mtDNA. Mitochondria were isolated from the skin of wild-type C57BL/6 mice exposed to 5kJ/m<sup>2</sup> of UVB radiation and the interaction between p53 and Pol $\gamma$  was assessed by co-immunoprecipitation with an antibody specific for p53 with subsequent detection of p53 or Pol $\gamma$  by Western analysis. As shown in Fig. 3A, Pol $\gamma$  and p53 proteins pulled down from the mitochondrial lysates by both p53 and Pol $\gamma$  antibodies increased at 1 hr and 24 hr after UVB treatment. We also determined UVB-induced p53 and mtDNA interaction by isolating mtDNA from the skin of C57BL/6 wild-type mice exposed to 5kJ/m<sup>2</sup> of UVB radiation. The mtDNA immunoprecipitated with p53 antibody were purified and amplified by real-time PCR with primers specific for mtDNA D-loop region to probe the relationship between mtDNA and Pol $\gamma$  function. As shown in Fig. 3B, the amplification of the D-loop region of mtDNA immunoprecipitated by p53 antibody increased significantly at 1 hr and 24 hr after UVB treatment. To verify the role of p53 in mtDNA repair by Pol $\gamma$  after UVB treatment, mtDNA immunoprecipitation was performed on p53<sup>+/+</sup> and p53<sup>-/-</sup> mice at 1 hr and 24 hr after UVB treatment. As shown in Fig. 3C, the amplification of the D-loop region of mtDNA immunoprecipitated by Pol $\gamma$  antibody in p53<sup>+/+</sup> mice increased significantly at 1 hr and 24 hr after UVB treatment. The amplification level of the D-loop in p53<sup>-/-</sup> mice was lower than that in the p53<sup>+/+</sup> mice and did not change significantly in response to UVB treatment. Thus, the significant increase in amplification of the D-loop region after UVB treatment was limited to the p53<sup>+/+</sup> genotypes, suggesting a role for p53 in the interaction of Pol $\gamma$  with mtDNA.

### **UVB induces physical interaction of MnSOD with p53 and Pol $\gamma$ , and the effect of MnSOD on Pol $\gamma$ and mtDNA**

We have previously observed an interaction between p53 and MnSOD in the mitochondria of epidermal cells exposed to DMBA and TPA (Zhao *et al.*, 2002, Zhao *et al.*, 2005). To determine whether UVB causes p53 and MnSOD to interact in mitochondria, skin mitochondrial lysates from UVB-treated wild-type C57BL/6 mice were immunoprecipitated with p53 and MnSOD antibodies, respectively. As shown in Fig. 4A, the amount of MnSOD and p53 proteins pulled down from mitochondrial lysates by p53 and MnSOD antibodies increased at 1 hr and 24 hr after UVB treatment. Previous studies have demonstrated that MnSOD is an integral part of the nucleoid complex (Kienhofer *et al.*, 2009). Hence, we tested whether UVB induces MnSOD and Pol $\gamma$  interaction using co-immunoprecipitation. As shown in Fig. 4B, the amount of MnSOD and Pol $\gamma$  proteins pulled down from mitochondrial lysates by Pol $\gamma$  and MnSOD antibodies increased at 1 hr and 24 hr after UVB

treatment. We further used p53<sup>+/+</sup> and p53<sup>-/-</sup> mice to perform a co-immunoprecipitation study to determine whether UVB induces interaction between MnSOD and Pol $\gamma$  and whether it is dependent on p53. As shown in Fig. 4C, the amount of MnSOD and Pol $\gamma$  proteins pulled down from mitochondrial lysates by Pol $\gamma$  and MnSOD antibodies increased at 1 hr and 24 hr after UVB treatment in both genotypes. To assess the role of MnSOD in mtDNA and Pol $\gamma$  interaction after UVB treatment, mtDNA immunoprecipitation was performed on MnSOD<sup>+/+</sup> and MnSOD<sup>+/-</sup> mice. As shown in Fig. 4D, amplification of the D-loop region of mtDNA immunoprecipitated by the Pol $\gamma$  antibody resulted in more than 1.5 fold increase at 1 hr after UVB treatment in both genotypes, and when compared between the genotypes. Although the increase was less than 1.5 fold at 24 hr after UVB treatment in both genotypes, the increase was significant in the MnSOD<sup>+/+</sup> genotype at 24 hr after UVB treatment. The results suggest that MnSOD interacts with both p53 and Pol $\gamma$ , but the interaction between MnSOD and Pol $\gamma$  appears to be independent of p53. The results also show that MnSOD enhances the Pol $\gamma$ /mtDNA interaction 24 hr after UVB-irradiation, implying a role for MnSOD in maintaining Pol $\gamma$  activity.

### MnSOD deficiency enhances UVB-mediated Pol $\gamma$ inactivation

To determine whether UVB treatment induces an alteration in Pol $\gamma$  protein level in the mitochondria of MnSOD<sup>+/+</sup> and MnSOD<sup>+/-</sup> mice, Western blotting for Pol $\gamma$  protein was performed using skin mitochondrial lysates from UVB- treated wild-type C57BL/6 mice. As shown in Fig. 5A, there was no apparent change in the Pol $\gamma$  protein level at 1 hr and 24 hr after UVB treatment in either genotype. UVB induces OONO<sup>-</sup> production in skin by the reaction of NO<sup>\*</sup> with O<sub>2</sub><sup>\*-</sup> which nitrates proteins and that Pol $\gamma$  protein undergoes oxidative damage-induced inactivation (Graziewicz *et al.*, 2002, Wu *et al.*, 2010). Pol $\gamma$  reverse transcriptase activity assay was performed using the skin mitochondrial lysates from UVB-treated MnSOD<sup>+/+</sup> and MnSOD<sup>+/-</sup> mice to determine whether UVB treatment results in a change in Pol $\gamma$  activity in the mitochondria. As shown in Fig. 5B, Pol $\gamma$  reverse transcriptase activity decreased significantly in MnSOD<sup>+/-</sup> genotype at 1 hr and 24 hr after UVB treatment compared to MnSOD<sup>+/+</sup> mice, where a significant decrease in activity was observed only at 24 hr after UVB treatment. To determine whether UVB-induced Pol $\gamma$  inactivation is associated with nitration, we performed a co-immunoprecipitation study using 3-nitrotyrosine antibody. As shown in Fig. 5C & 5D, the amount of Pol $\gamma$  protein pulled down from the mitochondrial lysates by 3-nitrotyrosine antibody significantly increased at 1 hr and 24 hr after UVB treatment in MnSOD<sup>+/-</sup> mice. There was a significant difference between the genotypes at 24 hr after UVB treatment, as shown in Fig. 5D. These results suggest MnSOD may be important in preventing nitration and subsequent inactivation of Pol $\gamma$  after UV exposure.

### Mn<sup>III</sup>TE-2-PyP<sup>5+</sup> rescues Pol $\gamma$ from inactivation by UVB-mediated nitration

Previous studies have clearly established Mn<sup>III</sup>TE-2-PyP<sup>5+</sup> as a potent O<sub>2</sub><sup>\*-</sup> and OONO<sup>-</sup> scavenger (Batinic-Haberle *et al.*, 2010, Batinic-Haberle 2010). To test if Pol $\gamma$  could be rescued from UV-induced inactivation, MnSOD<sup>+/-</sup> mice were pre-treated twice daily with Mn<sup>III</sup>TE-2-PyP<sup>5+</sup> at 5mg/kg body weight in 250  $\mu$ l volume before UVB exposure. Pol $\gamma$  reverse transcriptase activity assay was performed in skin mitochondrial lysates from saline and Mn<sup>III</sup>TE-2-PyP<sup>5+</sup> treated MnSOD<sup>+/-</sup> mice after UVB exposure. As shown in Fig. 6A,

Author Manuscript

Pol $\gamma$  reverse transcriptase activity in Mn<sup>III</sup>TE-2-PyP<sup>5+</sup> pre-treated MnSOD<sup>+/-</sup> mice increased significantly at 24 hr after UVB treatment and compared with saline pre-treated MnSOD<sup>+/-</sup> mice. There was a significant decrease in activity in saline pre-treated MnSOD<sup>+/-</sup> mice at 24 hr after UVB treatment. To determine whether Mn<sup>III</sup>TE-2-PyP<sup>5+</sup> pre-treatment reduces UVB-mediated Pol $\gamma$  inactivation by nitration, co-immunoprecipitation was performed using 3-nitrotyrosine antibody. As shown in Fig. 6B, the amount of Pol $\gamma$  protein pulled down from the mitochondrial lysates by 3-nitrotyrosine antibody in saline pre-treated MnSOD<sup>+/-</sup> mice increased significantly at 1 hr and 24 hr after UVB treatment. There was no significant change in nitration levels in Mn<sup>III</sup>TE-2-PyP<sup>5+</sup> pre-treated MnSOD<sup>+/-</sup> mice. When compared with saline pre-treated MnSOD<sup>+/-</sup> mice, the decrease in nitration in Mn<sup>III</sup>TE-2-PyP<sup>5+</sup> pre-treatment was significant at 24 hr after UVB treatment, as shown in Fig. 6C.

## Author Manuscript

## Discussion

Author Manuscript

The present study demonstrates that UVB-induced mtDNA damage triggers p53 translocation to mitochondria, that mitochondrial p53 interacts with both mtDNA and Pol $\gamma$  after UVB exposure, and that the mtDNA/Pol $\gamma$  association is dependent on the availability of p53. These results support a previous report on the role of p53 in the mtDNA repair process (Achanta *et al.*, 2005, Bakhanashvili *et al.*, 2008). We have previously shown that oxidative stress induces p53 translocation to mitochondria and its subsequent interaction with MnSOD in a multistage chemical carcinogenesis model (Zhao *et al.*, 2002, Zhao *et al.*, 2005). The present study confirms these findings using UVB treatment to cause DNA damage, and extends to demonstrate that UVB treatment leads to increased interaction between MnSOD and Pol $\gamma$  and that the interaction between MnSOD and Pol $\gamma$  is p53 independent. These results suggest that MnSOD may participate in mtDNA repair processes by acting as a fidelity protein protecting the function of the major DNA repair enzyme in the mitochondria. This conclusion is supported by the findings that 1) MnSOD deficiency leads to a decrease in mtDNA-Pol $\gamma$  interaction and 2) inactivation of Pol $\gamma$  by nitration is prevented by treatment with Mn<sup>III</sup>TE-2-PyP<sup>5+</sup>, a potent peroxynitrite inhibitor. The findings of this study verify that MnSOD is an integral part of the nucleoid complex and extend to demonstrate that the antioxidant property of MnSOD serves to enhance the fidelity of mtDNA repair by salvaging the DNA polymerase (Pol $\gamma$ ) in mitochondria from UV-induced peroxynitrite mediated inactivation.

Author Manuscript

Skin is the primary target of UVB radiation. UVB exposure has wide-ranging effects in skin, such as erythema and epidermal hyperplasia, which can eventually lead to photocarcinogenesis or photoaging. The underlying cellular processes for these conditions include DNA damage, apoptosis and oxidative stress. Both nuclear and mitochondrial DNA can be damaged by UVB radiation. Owing to its uniqueness, mtDNA has been used as a reliable biomarker for UV-induced DNA damage (Birch-machin *et al.*, 1998, Harbottle and Birch-Machin 2006, Krishnan *et al.*, 2004). Our Q-PCR analysis of mitochondrial genome indicates that UVB causes damage to mtDNA in mouse skin. The relative amplification ratio of the 10 kb mtDNA fragment at 1 hr and 24 hr after UVB treatment was significantly less than that of the reference control, which indicates the presence of DNA damage that blocks the amplification process. There were 0.15 lesions per 10 kb per strand at both the 1 hr and

24 hr treatments compared to the reference control. An earlier report that used Q-PCR to analyze UVB-exposed epidermal mtDNA from human skin shows deletions ranging from 4 to 10.5 kb in a 11.1 kb PCR fragment (Ray *et al.*, 2000). Thus, in our model UVB-induced mtDNA damage is being repaired.

UVB-induced oxidative stress and DNA damage stabilize p53 protein in the skin, leading to DNA repair in proliferating basal keratinocytes but cell cycle arrest and apoptosis in differentiated keratinocytes (Berg *et al.*, 1996, Li *et al.*, 1997, Ouhtit *et al.*, 2000, Renzing *et al.*, 1996, Tron *et al.*, 1998). UVB signature mutations in the p53 gene may lead to dysregulation of apoptosis and DNA repair, resulting in skin carcinogenesis (Li *et al.*, 1995a). Our results demonstrating p53-dependent UVB-induced mtDNA repair are consistent with these findings. The increased physical interaction of p53 with mtDNA and Pol $\gamma$  might be a p53 response to mtDNA damage after UVB treatment. A basal level of interaction between mtDNA and Pol $\gamma$  has been observed in both p53<sup>+/+</sup> and p53<sup>-/-</sup> genotypes. This interaction can be attributed to a p53-independent mtDNA replication process, since the very same basal level interaction between mtDNA and Pol $\gamma$  was observed 1 hr and 24 hr after UVB treatment in the p53<sup>-/-</sup> phenotype. In contrast, increased interaction between mtDNA and Pol $\gamma$  was observed 1 hr and 24 hr after UVB treatment in p53<sup>+/+</sup> mice. This increase from basal level can be attributed to mtDNA repair and indicates that the interaction requires p53. The presence of p53 enhances the accuracy of mtDNA repair by proof reading and by reducing the misincorporation of dNTP into mtDNA by Pol $\gamma$  (Bakhanashvili *et al.*, 2008). Recent studies have identified p53-regulated p53R2 as a subunit of ribonucleotide reductase (RNR), a rate-limiting enzyme in the de novo synthesis of deoxyribonucleotides (dNTPs) (Bourdon *et al.*, 2007, Kulawiec *et al.*, 2009, Lebedeva *et al.*, 2009). The UVB induced p53 stabilization triggers transcriptional up-regulation of p53R2, and increases output of dNTPs required for the UVB induced mtDNA repair process. This may be attributed to the increase in amplification of the D-loop region after UVB treatment observed in Fig. 3B.

The diverse functions of mitochondrial p53, which range from maintaining mtDNA integrity to apoptosis, led us to further explore our previous finding concerning MnSOD and p53 interaction in mitochondria. The physical interaction between p53 and MnSOD is observed with UVB treatment as was seen in chemical carcinogenesis studies. In light of new evidence that establishes MnSOD as an integral component of nucleoids (Kienhofer *et al.*, 2009), and our findings that a physical interaction occurs between MnSOD and Pol $\gamma$  after UVB treatment and that this interaction is p53-independent, these results suggest that MnSOD may enhance mtDNA stability by serving as a fidelity protein protecting the function of the key mitochondrial DNA repair enzyme. The interaction between MnSOD and Pol $\gamma$  and subsequent protection of Pol $\gamma$  from UVB-induced inactivation support a new role for mitochondrial antioxidant enzyme MnSOD in maintaining mtDNA fidelity. Our previous studies with MnSOD overexpressing and knockdown mice treated with DMBA/TPA have clearly established that MnSOD prevents protein oxidation in mitochondria (Zhao *et al.*, 2001, Zhao *et al.*, 2002). The decrease in the interaction between mtDNA and Pol $\gamma$  after UVB treatment in MnSOD<sup>+/-</sup> mice might be attributed to increased oxidative modification of Pol $\gamma$ . Oxidative stress in yeast due to a lack of MnSOD leads to

oxidation of various mitochondrial proteins such as aconitase, pyruvate, keto-acid dehydrogenase reductoisomerase, acetolactate synthase,  $\alpha$ -ketoglutarate dehydrogenase, HSP60, glyceraldehyde-3-phosphate, and cytosolic fatty acid synthase (Cabiscol *et al.*, 2000, O'Brien *et al.*, 2004). The Pol $\gamma$  protein is known to be sensitive to oxidative modification when exposed to hydrogen peroxide (Graziewicz *et al.*, 2002). The Pol $\gamma$  exonuclease proof reading mutator mice have increased point mutations, mtDNA deletions, and increased apoptosis that leads to accelerated aging (Kujoth *et al.*, 2005, Trifunovic *et al.*, 2004, Vermulst *et al.*, 2008). NO $\cdot$  and O $_2^{\cdot-}$  generated by UVB can result in OONO $^-$  production in skin, leading to nitration of proteins (Wu *et al.*, 2010). In this study we provide evidence for the first time that Pol $\gamma$  nitration and the consequent inactivation after UVB exposure are enhanced when MnSOD is deficient, and that pre-treatment of MnSOD with Mn<sup>III</sup>TE-2-PyP<sup>5+</sup> results in decreased nitration and inactivation of Pol $\gamma$ .

In summary, our study shows that MnSOD plays an important role in protecting the fidelity of mtDNA against UVB-induced mtDNA damage in keratinocytes. We propose a model in Fig. 7 to illustrate a novel dual-step strategy adapted by keratinocytes in response to UVB insult that enhances the repair of mtDNA and protects the mtDNA repair enzyme from being inactivated. On one hand, UVB-induced mtDNA damage triggers p53 translocation to mitochondria. The mitochondrial p53 interacts with mtDNA and enhances the polymerase and exonuclease activities of Pol $\gamma$ , which plays a major role in the mtDNA repair process with its proof reading ability. On the other hand, mitochondrial antioxidant MnSOD plays a novel role by interacting with Pol $\gamma$  and protecting it from peroxynitrite-mediated inactivation. Circumstances that lead to increased oxidative stress by depleting MnSOD level and/or decrease MnSOD activity by acetylation can result in Pol $\gamma$  inactivation. Increasing MnSOD levels and/or activity by Sirt3 deacetylation enhances mitochondrial O $_2^{\cdot-}$  scavenging and reduces ROS-mediated insult on vital mitochondrial proteins such as Pol $\gamma$ . Additional studies aimed at identification of the specific tyrosine residues of Pol $\gamma$  that are nitrated after UVB exposure, tyrosine residues that are responsible for reduced Pol $\gamma$  activity and/or protected by MnSOD will provide further biochemical insight into the mechanisms by which the nuclear encoded, mitochondrial localized protein, MnSOD, serves to maintain the fidelity of the mtDNA and will establish a nuclear mitochondrial feed forward loop in cellular adaptive responses against oxidative stress mediated mitochondrial DNA instability.

## Material and Methods

### Materials

All chemicals and reagents were purchased from Sigma-Aldrich (St. Louis, MO) with exception of the following: protease inhibitor set III from Calbiochem (La Jolla, CA), dithiothreitol from BioRad (Carlsbad, CA), rabbit poly-clonal anti-MnSOD from Upstate Technology (Lake Placid, NY), Protein A/G agarose from Santa Cruz Biotechnology (Santa Cruz, CA), rabbit poly-clonal anti-nitrotyrosine antibody from Cayman Chemical (Ann Arbor, MI), rabbit poly-clonal anti-Pol $\gamma$  antibody from Pierce Biotechnology (Rockford, IL), Monoclonal p53 antibody (DO-1) from Santa Cruz Biotechnology (Santa Cruz, CA),

poly(rA).oligo(dT)<sub>12-18</sub> from Midland Certified Reagent Company (Midland, TX), and DNase I from New England Biolabs Inc. (Ipswich, MA).

### Animal studies

Heterozygous MnSOD knockdown mice (MnSOD<sup>+/-</sup>) (Li *et al.*, 1995b, Van Remmen *et al.*, 1999) and p53 knock-out mice (p53<sup>-/-</sup>) (Jacks *et al.*, 1994) were generated and genotyped as described. The animal experimental procedures used in this study were approved by the Institutional Animal Care and Use Committee of the University of Kentucky.

### UV exposure

Depilated mice in resting phase of hair cycle and JB6 cells were exposed to ultraviolet irradiation in a Plexiglass cabinet (Plastic Design Corporation, MA). A single dose of 5kJ/m<sup>2</sup> (mice) or 400mJ/cm<sup>2</sup> (JB6 cells) was delivered by UVB lamps (Black light blue lamp, Sankyo Denko Ltd., Japan). The UV emittance was measured using a UVB photometer radiometer (International Light Technologies, Peabody, MA) equipped with UVB measuring head.

### Isolation of mitochondrial fraction from mouse skin tissue

The skin mitochondria were isolated as previously described (Zhao *et al.*, 2002).

### mtDNA isolation and mtDNA damage analysis using quantitative PCR (Q-PCR)

The Q-PCR to analyze mtDNA damage using Pico-Green dye was performed as described previously (Kovalenko and Santos 2009). mtDNA was isolated from mouse skin tissue using a genomic DNA extraction kit (QIAGEN, Chatsworth, VA). The mtDNA and PCR products were quantified using the PicoGreen dsDNA Quantitation kit (Invitrogen Corp., Carlsbad, CA). The fluorescence values of PCR products from UVB-treated samples and the control samples were used to calculate relative amplification and lesion frequency.

### Mitochondrial fractionation

The subcellular fractionation of enriched mitochondria was performed as described previously (Mihara and Moll 2003). Briefly, mouse skin was homogenized with a polytron homogenizer in calcium reticulocyte buffer (10mM Tris pH 7.6, 1.5 mM CaCl<sub>2</sub>, 10 mM NaCl) and mixed with 2ml of ice-cold mannitol-sucrose buffer (210 mM mannitol, 70 mM sucrose, 5 mM EDTA, 5 mM Tris, pH 7.6). Two hundred microlitres of whole skin homogenate was stored at -20°C for further use. The remainder of the whole skin homogenate was centrifuged thrice at 1000 × g for 5 min at 4°C to clear nuclear, cytosolic and intact skin cell fraction. The mitochondria were isolated by discontinuous sucrose gradient centrifugation.

### Co-Immunoprecipitation

Immunoprecipitation was performed as previously described (Bonifacino *et al.*, 2001). Briefly, the protein A/G-agarose beads (40 µL) were conjugated overnight to Poly, MnSOD, p53 (DO-1), and 3-nitrotyrosine antibodies (3 µg) at 4°C in 0.5 mL ice-cold PBS. Appropriate control antibody was used as negative control. The mitochondrial pellets were

lysed in denaturing buffer 1% w/v sodium dodecyl sulfate (SDS), 50 mM Tris-HCl, pH 7.4, 10 mM dithiothreitol, 5 mM EDTA, 15 U/ml DNase I, and 1  $\mu$ L/mL Protease inhibition by heat at 95°C for 5 min and the DNA was sheared. After denaturation and shearing, 250–500  $\mu$ g of precleared mitochondrial protein were immunoprecipitated with antibody conjugated protein A/G-agarose beads with 10  $\mu$ L of 10% BSA incubated overnight at 4°C in tube rotator. The immunoprecipitates were analyzed with 4–10% gradient gel.

### mtDNA immunoprecipitation

The CHIP-IT system (Active Motif, Carlsbad, CA) was used to investigate the interaction of Pol $\gamma$ , MnSOD, p53 (DO-1) and mtDNA. Briefly, skin mtDNA exposed to UVB was immunoprecipitated with p53 and Pol $\gamma$  antibodies, and the mtDNA D-loop region was quantified by real-time PCR (LightCycler 480 Real-Time PCR System, Roche). The following primer sets were designed and used to amplify the mtDNA D-loop region: 5'-ACTATCCCCTTCCCCATTTG-3' and 5'-TGTTGGTCATGGGCTGATTA-3'. Equal amounts of mtDNA from each treatment were used as input loading control, and mtDNA pulled down by IgG served as the negative antibody control.

### Poly reverse transcriptase activity assay

The RNA-dependent DNA polymerase activity of Pol $\gamma$  was measured as described previously (Longley and Copeland 2002, Taanman *et al.*, 2010). Briefly, the mitochondrial lysates prepared in extraction buffer (100 mM NaCl, 25 mM HEPES-KOH pH 8.0, 1% v/v Triton-X 100) were assayed at 37°C for 10 min in 50  $\mu$ L reaction mixture with 10  $\mu$ g of the mitochondrial protein, 25 mM HEPES-KOH pH 8.0, 0.5 mM MnCl<sub>2</sub>, 100 mM NaCl, 2.5 mM  $\beta$ -mercaptoethanol, 50  $\mu$ g/mL poly(rA).oligo(dT)<sub>12–18</sub>, 100  $\mu$ g/mL acetylated bovine serum albumin (Ac-BSA), 0.1 mM aphidicolin, 500  $\mu$ g/mL RNasin® RNase inhibitor (Promega, Madison, WI) and 5  $\mu$ M [ $\alpha$ -<sup>32</sup>P]thymidine 5'-triphosphate (dTTP; specific activity: 5 Ci/mmol) (Amersham Corp., Piscataway, NJ). The reaction was stopped with 1.0 ml of stop solution (500 mM NaOH, 100 mM sodium pyro-phosphate, 0.1 mg/mL sonicated calf thymus DNA, 0.5 mg/ml BSA). The DNA precipitated with 20% TCA was filtered through GF/C filters and washed thrice with 1N HCl, rinsed with 95% ethanol and dried. The TCA-insoluble radioactivity was measured by liquid scintillation counting.

### Treatment with Mn-based porphyrin

The Mn(III) meso-tetrakis(*N*-ethylpyridinium-2-yl) porphyrin (Mn<sup>III</sup>TE-2-PyP<sup>5+</sup>) was synthesized as previously described (Batinic-Haberle *et al.*, 1999, Ferrer-Sueta *et al.*, 1999). The mice were injected IP with 5 mg/kg of Mn<sup>III</sup>TE-2-PyP<sup>5+</sup> in saline twice daily for 2 days before UVB treatment.

### Data analysis

The data are represented as mean  $\pm$  SEM from replicate samples (n = 3), and were analyzed by one-way and two-way analyses of variance using Prism software (GraphPad, San Diego, CA). An  $\alpha$  level of P<0.05 was considered significant.

## Acknowledgments

This work was supported by the National Institutes of Health (RO1CA073599-11).

## References

- Achanta G, Sasaki R, Feng L, Carew JS, Lu W, Pelicano H, et al. Novel role of p53 in maintaining mitochondrial genetic stability through interaction with DNA Pol  $\gamma$ . *EMBO J*. 2005; 24:3482–3492. [PubMed: 16163384]
- Aitken GR, Henderson JR, Chang SC, McNeil CJ, Birch-Machin MA. Direct monitoring of UV-induced free radical generation in HaCaT keratinocytes. *Clin Exp Dermatol*. 2007; 32:722–727. [PubMed: 17953641]
- Alvarez B, Radi R. Peroxynitrite reactivity with amino acids and proteins. *Amino Acids*. 2003; 25:295–311. [PubMed: 14661092]
- Bakhanashvili M, Grinberg S, Bonda E, Simon AJ, Moshitch-Moshkovitz S, Rahav G. p53 in mitochondria enhances the accuracy of DNA synthesis. *Cell Death Differ*. 2008; 15:1865–1874. [PubMed: 19011642]
- Batinic-Haberle I, Spasojevic I, Hambright P, Benov L, Crumbliss AL, Fridovich I. Relationship among Redox Potentials, Proton Dissociation Constants of Pyrrolic Nitrogens, and in Vivo and in Vitro Superoxide Dismutating Activities of Manganese(III) and Iron(III) Water-Soluble Porphyrins. *Inorg Chem*. 1999; 38:4011–4022.
- Batinic-Haberle I, Reboucas JS, Spasojevic I. Superoxide dismutase mimics: chemistry, pharmacology, and therapeutic potential. *Antioxid Redox Signal*. 2010; 13:877–918. [PubMed: 20095865]
- Batinic-Haberle, IR.; Benov, JSL.; Spasojevic, I. In *Handbook of Porphyrin Science*. Vol. Part 2. World Scientific; Singapore: 2010. *Catalysis and Bio-Inspired Systems*; p. 291-393.
- Berg RJ, van Kranen HJ, Rebel HG, de Vries A, van Vloten WA, Van Kreijl CF, et al. Early p53 alterations in mouse skin carcinogenesis by UVB radiation: immunohistochemical detection of mutant p53 protein in clusters of preneoplastic epidermal cells. *Proc Natl Acad Sci U S A*. 1996; 93:274–278. [PubMed: 8552621]
- Bickers DR, Athar M. Oxidative Stress in the Pathogenesis of Skin Disease. *J Invest Dermatol*. 2006; 126:2565–2575. [PubMed: 17108903]
- Birch-machin MA, Tindall M, Turner R, Haldane F, Rees JL. Mitochondrial DNA Deletions in Human Skin Reflect Photo- Rather Than Chronologic Aging. *J Invest Dermatol*. 1998; 110:149–152. [PubMed: 9457910]
- Bogenhagen DF, Pinz KG, Perez-Jannotti RM. Enzymology of mitochondrial base excision repair. *Prog Nucleic Acid Res Mol Biol*. 2001:257–271. [PubMed: 11554302]
- Bolden A, Noy GP, Weissbach A. DNA polymerase of mitochondria is a gamma-polymerase. *J Biol Chem*. 1977; 252:3351–3356. [PubMed: 16896]
- Bonifacino JS, Dell'Angelica EC, Springer TA. Immunoprecipitation. *Curr Protoc Mol Biol*. 2001; Chapter 10(Unit 10):16. [PubMed: 18265056]
- Bourdon A, Minai L, Serre V, Jais JP, Sarzi E, Aubert S, et al. Mutation of RRM2B, encoding p53-controlled ribonucleotide reductase (p53R2), causes severe mitochondrial DNA depletion. *Nat Genet*. 2007; 39:776–780. [PubMed: 17486094]
- Brash DE, Rudolph JA, Simon JA, Lin A, McKenna GJ, Baden HP, et al. A role for sunlight in skin cancer: UV-induced p53 mutations in squamous cell carcinoma. *Proc Natl Acad Sci U S A*. 1991; 88:10124–10128. [PubMed: 1946433]
- Brown WM, George M, Wilson AC. Rapid Evolution of Animal Mitochondrial DNA. *Proc Natl Acad Sci U S A*. 1979; 76:1967–1971. [PubMed: 109836]
- Cabiscol E, Piulats E, Echave P, Herrero E, Ros J. Oxidative Stress Promotes Specific Protein Damage in *Saccharomyces cerevisiae*. *J Biol Chem*. 2000; 275:27393–27398. [PubMed: 10852912]
- Carrodeguas JA, Kobayashi R, Lim SE, Copeland WC, Bogenhagen DF. The Accessory Subunit of *Xenopus laevis* Mitochondrial DNA Polymerase gamma Increases Processivity of the Catalytic

Subunit of Human DNA Polymerase gamma and Is Related to Class II Aminoacyl-tRNA Synthetases. *Mol Cell Biol.* 1999; 19:4039–4046. [PubMed: 10330144]

Chen XJ, Butow RA. The organization and inheritance of the mitochondrial genome. *Nat Rev Genet.* 2005; 6:815–825. [PubMed: 16304597]

Decraene D, Smaers K, Gan D, Mammone T, Matsui M, Maes D, et al. A Synthetic Superoxide Dismutase Catalase Mimetic (EUK-134) Inhibits Membrane-Damage-Induced Activation of Mitogen-Activated Protein Kinase Pathways and Reduces p53 Accumulation in Ultraviolet B-Exposed Primary Human Keratinocytes. *J Investig Dermatol.* 2004; 122:484–491. [PubMed: 15009734]

Esworthy RS, Ho Y-S, Chu F-F. The Gpx1 Gene Encodes Mitochondrial Glutathione Peroxidase in the Mouse Liver. *Arch Biochem Biophys.* 1997; 340:59–63. [PubMed: 9126277]

Ferrer-Sueta G, Batinic-Haberle I, Spasojevic I, Fridovich I, Radi R. Catalytic scavenging of peroxynitrite by isomeric Mn(III) N-methylpyridylporphyrins in the presence of reductants. *Chem Res Toxicol.* 1999; 12:442–449. [PubMed: 10328755]

Garrido N, Griparic L, Jokitalo E, Wartiovaara J, van der Blik AM, Spelbrink JN. Composition and Dynamics of Human Mitochondrial Nucleoids. *Mol Biol Cell.* 2003; 14:1583–1596. [PubMed: 12686611]

Gray H, Wong TW. Purification and identification of subunit structure of the human mitochondrial DNA polymerase. *J Biol Chem.* 1992; 267:5835–5841. [PubMed: 1556099]

Graziewicz MA, Day BJ, Copeland WC. The mitochondrial DNA polymerase as a target of oxidative damage. *Nucl Acids Res.* 2002; 30:2817–2824. [PubMed: 12087165]

Graziewicz MA, Longley MJ, Bienstock RJ, Zeviani M, Copeland WC. Structure-function defects of human mitochondrial DNA polymerase in autosomal dominant progressive external ophthalmoplegia. *Nat Struct Mol Biol.* 2004; 11:770–776. [PubMed: 15258572]

Hall PA, McKee PH, Menage HD, Dover R, Lane DP. High levels of p53 protein in UV-irradiated normal human skin. *Oncogene.* 1993; 8:203–207. [PubMed: 8093810]

Harbottle A, Birch-Machin MA. Real-time PCR analysis of a 3895 bp mitochondrial DNA deletion in nonmelanoma skin cancer and its use as a quantitative marker for sunlight exposure in human skin. *Br J Cancer.* 2006; 94:1887–1893. [PubMed: 16721366]

Heyne K, Mannebach S, Wuertz E, Knaup KX, Mahyar-Roemer M, Roemer K. Identification of a putative p53 binding sequence within the human mitochondrial genome. *FEBS Lett.* 2004; 578:198–202. [PubMed: 15581641]

Holmgren A. Thioredoxin. *Annu Rev Biochem.* 1985; 54:237–271. [PubMed: 3896121]

Hubscher U, Kuenzle CC, Spadari S. Functional roles of DNA polymerases beta and gamma. *Proc Natl Acad Sci U S A.* 1979; 76:2316–2320. [PubMed: 287074]

Jacks T, Remington L, Williams BO, Schmitt EM, Halachmi S, Bronson RT, et al. Tumor spectrum analysis in p53-mutant mice. *Curr Biol.* 1994; 4:1–7. [PubMed: 7922305]

Johnson AA, Tsai Y-c, Graves SW, Johnson KA. Human Mitochondrial DNA Polymerase Holoenzyme: Reconstitution and Characterization. *Biochemistry.* 2000; 39:1702–1708. [PubMed: 10677218]

Kienhofer J, Haussler DJF, Ruckelshausen F, Muessig E, Weber K, Pimentel D, et al. Association of mitochondrial antioxidant enzymes with mitochondrial DNA as integral nucleoid constituents. *FASEB J.* 2009; 23:2034–2044. [PubMed: 19228881]

Kovalenko, OA.; Santos, JH. *Analysis of Oxidative Damage by Gene-Specific Quantitative PCR.* John Wiley & Sons, Inc; 2009.

Krishnan KJ, Harbottle A, Birch-Machin MA. The Use of a 3895 bp Mitochondrial DNA Deletion as a Marker for Sunlight Exposure in Human Skin. *J Investig Dermatol.* 2004; 123:1020–1024. [PubMed: 15610508]

Kujoth GC, Hiona A, Pugh TD, Someya S, Panzer K, Wohlgemuth SE, et al. Mitochondrial DNA Mutations, Oxidative Stress, and Apoptosis in Mammalian Aging. *Science.* 2005; 309:481–484. [PubMed: 16020738]

Kulawiec M, Ayyasamy V, Singh KK. p53 regulates mtDNA copy number and mitochkpoint pathway. *J Carcinog.* 2009; 8:8. [PubMed: 19439913]

- Lebedeva MA, Eaton JS, Shadel GS. Loss of p53 causes mitochondrial DNA depletion and altered mitochondrial reactive oxygen species homeostasis. *Biochim Biophys Acta*. 2009; 1787:328–334. [PubMed: 19413947]
- Legros F, Malka F, Frachon P, Lombes A, Rojo M. Organization and dynamics of human mitochondrial DNA. *J Cell Sci*. 2004; 117:2653–2662. [PubMed: 15138283]
- Lewis W, Day BJ, Kohler JJ, Hosseini SH, Chan SSL, Green EC, et al. Decreased mtDNA, oxidative stress, cardiomyopathy, and death from transgenic cardiac targeted human mutant polymerase  $\gamma$ . *Lab Invest*. 2006; 87:326–335. [PubMed: 17310215]
- Li G, Ho VC, Berean K, Tron VA. Ultraviolet Radiation Induction of Squamous Cell Carcinomas in p53 Transgenic Mice. *Cancer Res*. 1995a; 55:2070–2074. [PubMed: 7743504]
- Li G, Ho VC, Mitchell DL, Trotter MJ, Tron VA. Differentiation-dependent p53 regulation of nucleotide excision repair in keratinocytes. *Am J Pathol*. 1997; 150:1457–1464. [PubMed: 9095000]
- Li Y, Huang T-T, Carlson EJ, Melov S, Ursell PC, Olson JL, et al. Dilated cardiomyopathy and neonatal lethality in mutant mice lacking manganese superoxide dismutase. *Nat Genet*. 1995b; 11:376–381. [PubMed: 7493016]
- Lim SE, Ponamarev MV, Longley MJ, Copeland WC. Structural Determinants in Human DNA Polymerase  $\gamma$  Account for Mitochondrial Toxicity from Nucleoside Analogs. *J Mol Biol*. 2003; 329:45–57. [PubMed: 12742017]
- Liu M, Dhanwada KR, Birt DF, Hecht S, Pelling JC. Increase in p53 protein half-life in mouse keratinocytes following UV-B irradiation. *Carcinogenesis*. 1994; 15:1089–1092. [PubMed: 8020138]
- Longley MJ, Prasad R, Srivastava DK, Wilson SH, Copeland WC. Identification of 5′deoxyribose phosphate lyase activity in human DNA polymerase gamma and its role in mitochondrial base excision repair in vitro. *Proc Natl Acad Sci U S A*. 1998; 95:12244–12248. [PubMed: 9770471]
- Longley MJ, Copeland WC. Purification, separation, and identification of the human mtDNA polymerase with and without its accessory subunit. *Methods Mol Biol*. 2002; 197:245–257. [PubMed: 12013800]
- Maglio DHG, Paz ML, Ferrari A, Weill FS, Czerniczyniec A, Leoni J, et al. Skin damage and mitochondrial dysfunction after acute ultraviolet B irradiation: relationship with nitric oxide production. *Photodermatol Photoimmunol Photomed*. 2005; 21:311–317. [PubMed: 16313242]
- Melov S, Coskun P, Patel M, Tuinstra R, Cottrell B, Jun AS, et al. Mitochondrial disease in superoxide dismutase 2 mutant mice. *Proc Natl Acad Sci U S A*. 1999; 96:846–851. [PubMed: 9927656]
- Mihara M, Erster S, Zaika A, Petrenko O, Chittenden T, Pancoska P, et al. p53 Has a Direct Apoptogenic Role at the Mitochondria. *Mol Cell*. 2003; 11:577–590. [PubMed: 12667443]
- Mihara M, Moll UM. Detection of mitochondrial localization of p53. *Methods Mol Biol*. 2003; 234:203–209. [PubMed: 12824533]
- O’Brien KM, Dirmeier R, Engle M, Poyton RO. Mitochondrial Protein Oxidation in Yeast Mutants Lacking Manganese-(MnSOD) or Copper- and Zinc-containing Superoxide Dismutase (CuZnSOD). *J Biol Chem*. 2004; 279:51817–51827. [PubMed: 15385544]
- Ouhtit A, Muller HK, Davis DW, Ullrich SE, McConkey D, Ananthaswamy HN. Temporal Events in Skin Injury and the Early Adaptive Responses in Ultraviolet-Irradiated Mouse Skin. *Am J Pathol*. 2000; 156:201–207. [PubMed: 10623668]
- Ozden O, Park SH, Kim HS, Jiang H, Coleman MC, Spitz DR, et al. Acetylation of MnSOD directs enzymatic activity responding to cellular nutrient status or oxidative stress. *Aging (Albany NY)*. 2011; 3:102–107. [PubMed: 21386137]
- Ray AJ, Turner R, Nikaido O, Rees JL, Birch-Machin MA. The Spectrum of Mitochondrial DNA Deletions is a Ubiquitous Marker of Ultraviolet Radiation Exposure in Human Skin. *J Invest Dermatol*. 2000; 115:674–679. [PubMed: 10998142]
- Renzing J, Hansen S, Lane D. Oxidative stress is involved in the UV activation of p53. *J Cell Sci*. 1996; 109:1105–1112. [PubMed: 8743957]
- Shokolenko I, Venediktova N, Bochkareva A, Wilson GL, Alexeyev MF. Oxidative stress induces degradation of mitochondrial DNA. *Nucl Acids Res*. 2009; 37:2539–2548. [PubMed: 19264794]

- Stuart JA, Karahalil B, Hogue BA, Souza-Pinto NC, Bohr VA. Mitochondrial and nuclear DNA base excision repair are affected differently by caloric restriction. *FASEB J*. 2004;03–0890fje.
- Taanman JW, Heiske M, Letellier T. Measurement of kinetic parameters of human platelet DNA polymerase gamma. *Methods*. 2010; 51:374–378. [PubMed: 20227504]
- Tao R, Coleman MC, Pennington JD, Ozden O, Park SH, Jiang H, et al. Sirt3-mediated deacetylation of evolutionarily conserved lysine 122 regulates MnSOD activity in response to stress. *Mol Cell*. 2010; 40:893–904. [PubMed: 21172655]
- Trifunovic A, Wredenberg A, Falkenberg M, Spelbrink JN, Rovio AT, Bruder CE, et al. Premature ageing in mice expressing defective mitochondrial DNA polymerase. *Nature*. 2004; 429:417–423. [PubMed: 15164064]
- Tron VA, Trotter MJ, Tang L, Krajewska M, Reed JC, Ho VC, et al. p53-Regulated Apoptosis Is Differentiation Dependent in Ultraviolet B-Irradiated Mouse Keratinocytes. *Am J Pathol*. 1998; 153:579–585. [PubMed: 9708817]
- Van Goethem G, Dermaut B, Lofgren A, Martin J-J, Van Broeckhoven C. Mutation of POLG is associated with progressive external ophthalmoplegia characterized by mtDNA deletions. *Nat Genet*. 2001; 28:211–212. [PubMed: 11431686]
- Van Remmen H, Salvador C, Yang H, Huang TT, Epstein CJ, Richardson A. Characterization of the Antioxidant Status of the Heterozygous Manganese Superoxide Dismutase Knockout Mouse. *Arch Biochem Biophys*. 1999; 363:91–97. [PubMed: 10049502]
- Vaseva AV, Moll UM. The mitochondrial p53 pathway. *Biochim Biophys Acta*. 2009; 1787:414–420. [PubMed: 19007744]
- Vermulst M, Wanagat J, Kujoth GC, Bielas JH, Rabinovitch PS, Prolla TA, et al. DNA deletions and clonal mutations drive premature aging in mitochondrial mutator mice. *Nat Genet*. 2008; 40:392–394. [PubMed: 18311139]
- Waster PK, Ollinger KM. Redox-Dependent Translocation of p53 to Mitochondria or Nucleus in Human Melanocytes after UVA- and UVB-Induced Apoptosis. *J Invest Dermatol*. 2009; 129:1769–1781. [PubMed: 19158844]
- Weisiger RA, Fridovich I. Superoxide dismutase. Organelle specificity. *J Biol Chem*. 1973; 248:3582–3592. [PubMed: 4702877]
- Wu S, Wang L, Jacoby AM, Jasinski K, Kubant R, Malinski T. Ultraviolet B Light-induced Nitric Oxide/Peroxynitrite Imbalance in Keratinocytes—Implications for Apoptosis and Necrosis. *Photochem Photobiol*. 2010; 86:389–396. [PubMed: 20074088]
- Yakes FM, Van Houten B. Mitochondrial DNA damage is more extensive and persists longer than nuclear DNA damage in human cells following oxidative stress. *Proc Natl Acad Sci U S A*. 1997; 94:514–519. [PubMed: 9012815]
- Yakubovskaya E, Chen Z, Carrodegua JA, Kisker C, Bogenhagen DF. Functional Human Mitochondrial DNA Polymerase  $\gamma$  Forms a Heterotrimer. *J Biol Chem*. 2006; 281:374–382. [PubMed: 16263719]
- Zhao Y, Xue Y, Oberley TD, Kiningham KK, Lin S-M, Yen H-C, et al. Overexpression of Manganese Superoxide Dismutase Suppresses Tumor Formation by Modulation of Activator Protein-1 Signaling in a Multistage Skin Carcinogenesis Model. *Cancer Res*. 2001; 61:6082–6088. [PubMed: 11507057]
- Zhao Y, Oberley TD, Chaiswing L, Lin SM, Epstein CJ, Huang TT, et al. Manganese superoxide dismutase deficiency enhances cell turnover via tumor promoter-induced alterations in AP-1 and p53-mediated pathways in a skin cancer model. *Oncogene*. 2002; 21:3836–3846. [PubMed: 12032821]
- Zhao Y, Chaiswing L, Velez JM, Batinic-Haberle I, Colburn NH, Oberley TD, et al. p53 Translocation to Mitochondria Precedes Its Nuclear Translocation and Targets Mitochondrial Oxidative Defense Protein-Manganese Superoxide Dismutase. *Cancer Res*. 2005; 65:3745–3750. [PubMed: 15867370]

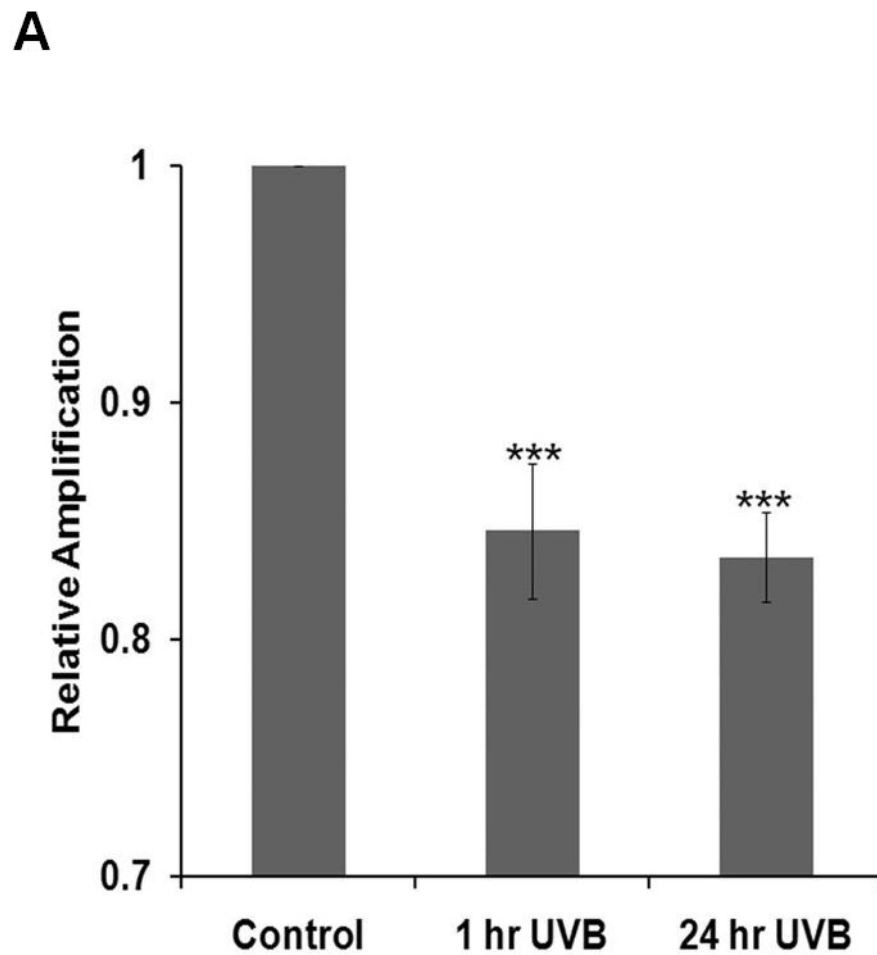


**Figure 1. Quantification of mtDNA damage in mouse skin induced by UVB radiation**

Wild-type C57BL/6 mice were exposed to  $5\text{kJ/m}^2$  of UVB radiation. mtDNA was isolated and analyzed with Q-PCR using primers specific for mouse mtDNA. The 10 kb mtDNA fragment was amplified and the blockage of rTth DNA polymerase amplification by damage in mtDNA was quantified in PCR products with Pico-Green dye. The relative amplification levels at 1 hr and 24 hr after UVB treatment were normalized with untreated control. \*\*\* $P < 0.001$  compared with control.

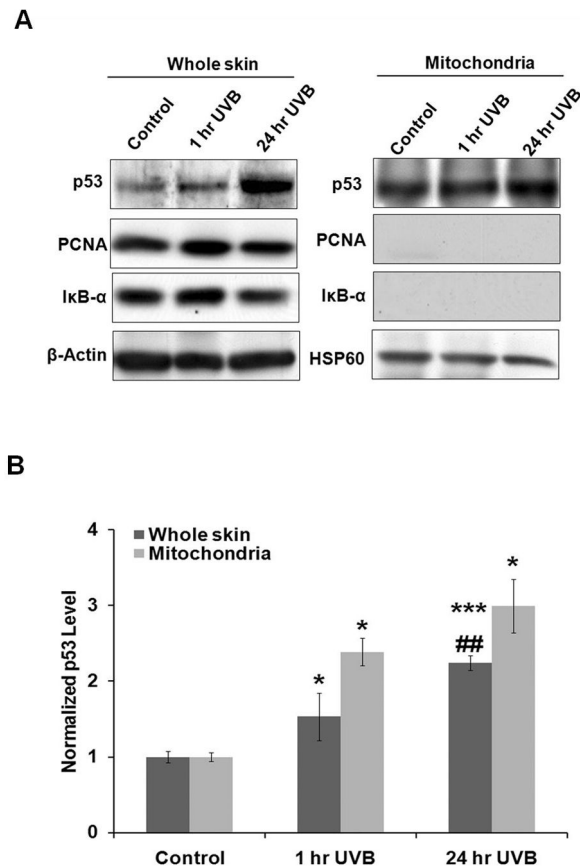


**Figure 2. UVB enhances p53 mitochondrial translocation**

(A) C57BL/6 mice were exposed to  $5\text{kJ/m}^2$  of UVB radiation. Whole skin tissue lysates and fractionated mitochondrial lysates were immunoblotted for p53 antibody (DO-1). Ponceau staining was used to confirm equal loading and uniform transfer of protein. Monoclonal anti- $\beta$ -actin and anti-HSP60 antibodies were used as internal loading control. (B) The p53 accumulations in whole skin lysates and mitochondrial lysates at 1 hr and 24 hr after UVB exposure were quantified. Results were averaged from 3 sets of independent experiments. \* $P < 0.05$ , \*\*\* $P < 0.001$ , compared with control, ## $P < 0.01$ , comparison of 1 hr and 24 hr UVB treatment.

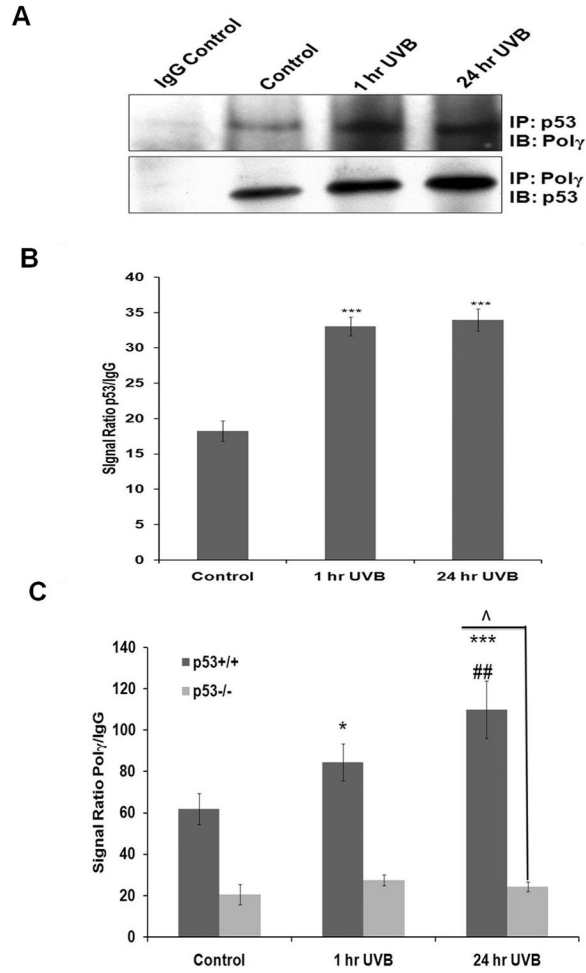


**Figure 3. UVB-induced physical interaction of p53-Poly-mtDNA**

(A) Skin mitochondrial lysates from wild-type C57BL/6 mice exposed to 5kJ/m<sup>2</sup> of UVB radiation were immunoprecipitated with p53 (DO-1), Polyγ antibodies, and control IgG. (B) mtDNA isolated from wild-type C57BL/6 mice skin exposed or sham exposed to 5 kJ/m<sup>2</sup> of UVB radiation was immunoprecipitated with p53 antibody (DO-1) and control IgG. The input mtDNA from control at 1 hr and 24 hr after UVB treatment was used as internal control. Real-Time PCR was used to amplify mtDNA D-loop region from input and immunoprecipitated mtDNA. \*\*\*P < 0.001. (C) mtDNA isolated from p53<sup>+/+</sup> and p53<sup>-/-</sup> mice skin exposed or not exposed to 5kJ/m<sup>2</sup> of UVB radiation was immunoprecipitated with Polyγ antibody. Real-time PCR was used to amplify the immunoprecipitated mtDNA D-loop. \*P < 0.05, \*\*\*P < 0.001, compared with control; ##P < 0.01, compared at 1 hr and 24 hr after UVB treatment; ^P < 0.05, compared between p53<sup>+/+</sup> and p53<sup>-/-</sup> genotypes.

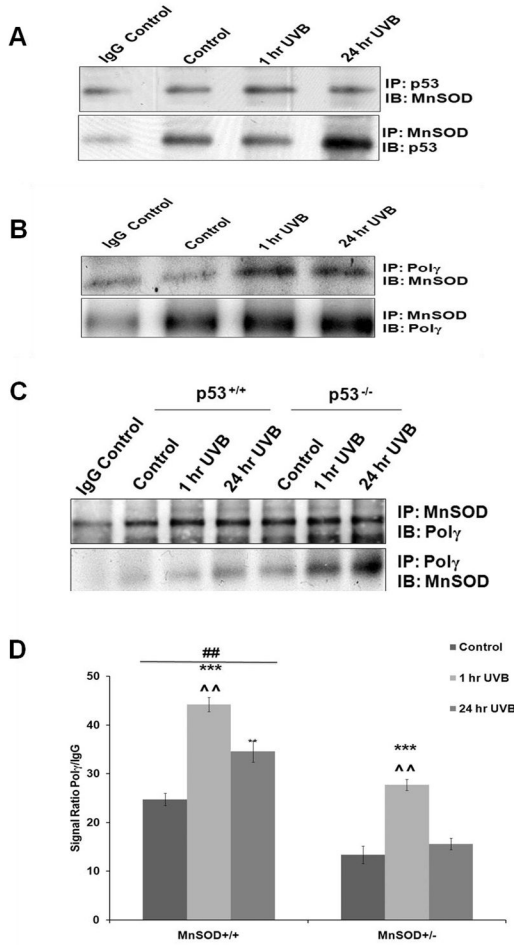


**Figure 4. UVB-induced physical interaction of MnSOD-p53-Poly**  
**(A)** Skin mitochondrial lysates from wild-type C57BL/6 mice exposed to 5kJ/m<sup>2</sup> of UVB radiation were immunoprecipitated with p53 (DO-1), MnSOD antibodies, and control IgG. Co-immunoprecipitated MnSOD and p53 were quantified by immunoblotting with specific antibodies. **(B)** Co-immunoprecipitation of Poly and MnSOD. Mitochondrial lysates from mice skin exposed to UVB at 1 hr and 24 hr were immunoprecipitated with Poly, MnSOD antibodies, and control IgG. Co-immunoprecipitated Poly and MnSOD were quantified by immunoblotting with specific antibodies. **(C)** Mitochondrial lysates from p53<sup>+/+</sup> and p53<sup>-/-</sup> mice skin exposed to UVB were immunoprecipitated with Poly, MnSOD antibodies and control IgG. Co-immunoprecipitated Poly and MnSOD were quantified by immunoblotting with specific antibodies. **(D)** mtDNA isolated from MnSOD<sup>+/+</sup> and MnSOD<sup>+/-</sup> mice skin exposed to 5kJ/m<sup>2</sup> of UVB radiation was immunoprecipitated with Poly antibody. Real-time PCR was used to amplify the precipitated mtDNA D-loop. \*\*\*P < 0.001, \*\*P < 0.01, compared with control; ^P < 0.01 compared at 1 hr and 24 hr after UVB treatment; ##P < 0.01 compared between MnSOD<sup>+/+</sup> and MnSOD<sup>+/-</sup> mice.

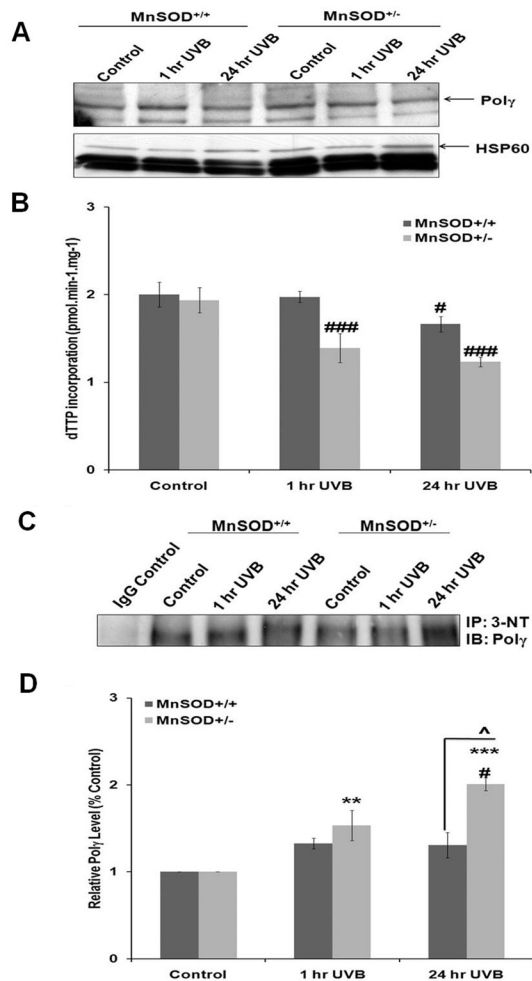


### Figure 5. UVB induced Poly inactivation by nitration

(A) Immunoblot analysis of Poly protein levels in MnSOD<sup>+/+</sup> and MnSOD<sup>+/-</sup> mice skin mitochondria exposed to 5kJ/m<sup>2</sup> of UVB radiation. (B) Poly reverse transcriptase activity assay in MnSOD<sup>+/+</sup> and MnSOD<sup>+/-</sup> mice skin mitochondria exposed or not exposed to 5 kJ/m<sup>2</sup> of UVB radiation #P < 0.05, ###P < 0.001 compared with control. (C) MnSOD<sup>+/+</sup> and MnSOD<sup>+/-</sup> mouse skin exposed to 5 kJ/m<sup>2</sup> of UVB radiation was co-immunoprecipitated with 3-nitrotyrosine antibody. Co-immunoprecipitates were immunoblotted with Poly antibody. (D) Quantification of Poly co-immunoprecipitation by 3-nitrotyrosine antibody. \*\*P < 0.01, \*\*\*P < 0.001 compared with control; #P < 0.05 compared between 1 hr and 24 hr after UVB treatment; ^P < 0.05 compared between MnSOD<sup>+/+</sup> and MnSOD<sup>+/-</sup> mice.

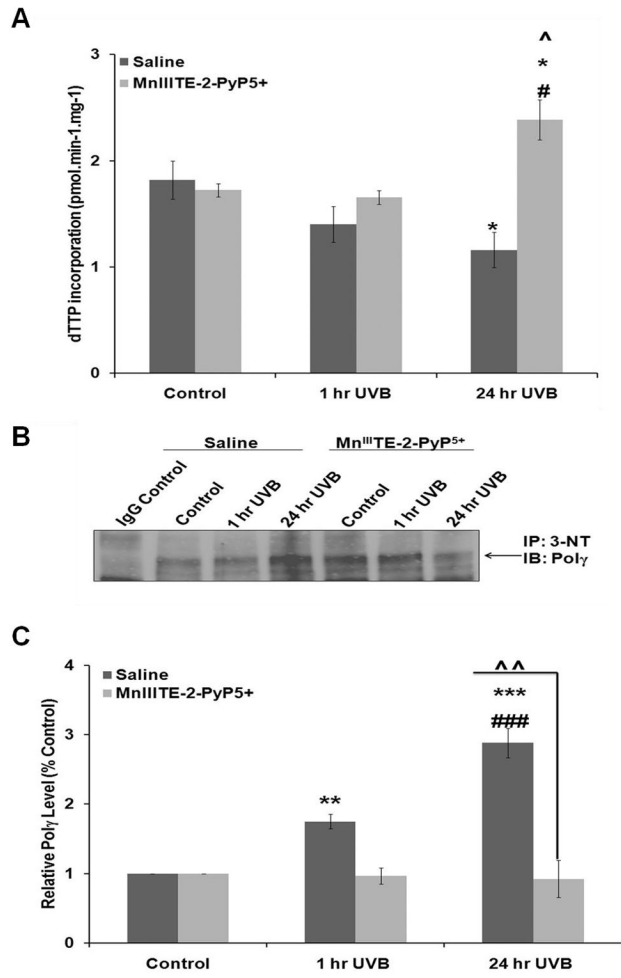


**Figure 6. Mn<sup>III</sup>TE-2-PyP<sup>5+</sup> protects UVB induced Poly inactivation by nitration in MnSOD<sup>+/-</sup> mice**

(A) Poly reverse transcriptase activity assay in Mn<sup>III</sup>TE-2-PyP<sup>5+</sup> and saline pre-treated MnSOD<sup>+/-</sup> mice skin mitochondria exposed to 5 kJ/m<sup>2</sup> of UVB radiation \*P < 0.05 compared with control; #P < 0.05 compared between 1 hr and 24 hr after UVB treatment; ^P < 0.05 compared between Mn<sup>III</sup>TE-2-PyP<sup>5+</sup> and saline pre-treatment. (B) Mn<sup>III</sup>TE-2-PyP<sup>5+</sup> and saline pre-treated MnSOD<sup>+/-</sup> mice skin exposed to 5 kJ/m<sup>2</sup> of UVB radiation were co-immunoprecipitated with 3-nitrotyrosine antibody and immunoblotted with Poly antibody. (C) Quantification of Poly co-immunoprecipitation by anti-3-nitrotyrosine antibody in Mn<sup>III</sup>TE-2-PyP<sup>5+</sup> and saline pre-treated MnSOD<sup>+/-</sup> mice skin exposed to 5 kJ/m<sup>2</sup> of UVB radiation. \*\*P < 0.01, \*\*\*P < 0.001 compared with control; ###P < 0.001 compared between 1 hr and 24 hr after UVB treatment; ^^P < 0.01 compared between Mn<sup>III</sup>TE-2-PyP<sup>5+</sup> and saline pre-treatment.

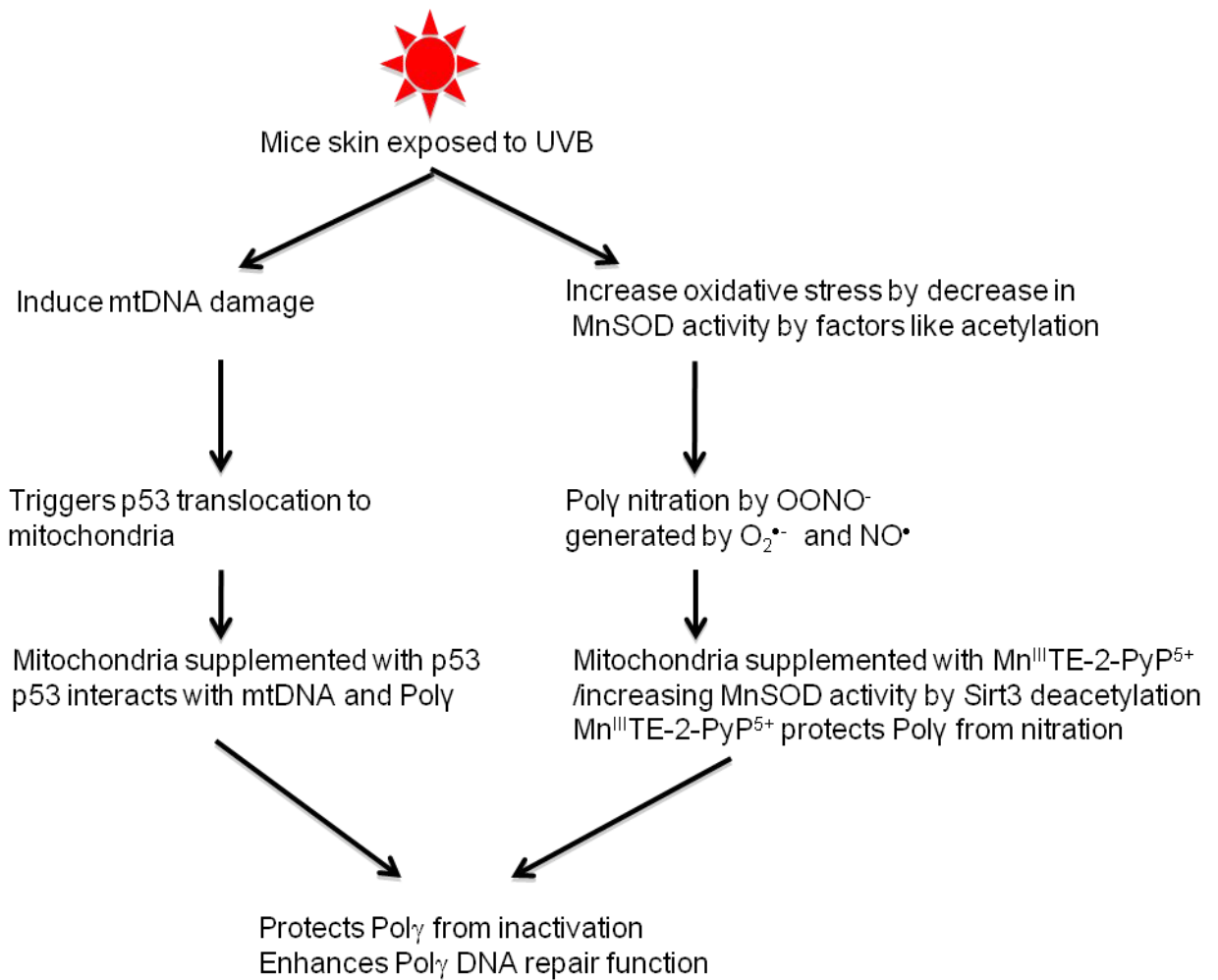


**Figure 7.** Schematic illustration of novel dual-step strategy adapted by keratinocytes to survive UVB insult

**Table 1**  
**The number of lesions per 10 kb mtDNA at 1 hr and 24 hr after UVB treatment was quantified after normalizing with mitochondrial copy number**

Quantitative analysis of mtDNA lesions induced by UVB

	Control	1 hr UVB	24 hr UVB
Lesions/10kb	0	0.17 ± 0.03 **	0.18 ± 0.002 ****

The data are presented as mean ± S.E. and n = 4,

\*\* P < 0.01,

\*\*\*\* P < 0.001 compared with control.